International Journal of Automotive Technology, Vol. 24, No. 4, pp. 1205-1211 (2023)
DOI 10.1007/s12239–023–0098–2

pISSN 1229–9138/ eISSN 1976–3832

DEVELOPMENT OF A NEW MEASUREMENT SYSTEM FOR PISTON RING FRICTION BASED ON THE FLOATING LINER METHOD

Hyunjung Oh[1)], Kyoung-Pyo Ha[2)] and Kyoungdoug Min[1)*]

[1)]School of Mechanical Engineering, Seoul National University, Seoul 08826, Korea
[2)]Hyundai America Technical Center Inc., 6800 Geddes Rd. Superior Township, MI 48198, USA

(Received 20 April 2022; Revised 24 April 2023; Accepted 30 May 2023)

ABSTRACT–A new friction measurement system was developed to investigate piston ring friction in detail based on the floating liner method. Unlike the conventional floating liner experiments, an extended piston was adopted for the conventional crank-piston system to minimize friction from a piston lateral motion. The interaction between piston skirt and liner caused by piston thrust force can be excluded with the new measurement system. Therefore, a parametric study for the only piston ring friction can be possible. In this study, the experiments were conducted under both motoring and firing conditions. The oil temperature was changed to observe the effect of the oil viscosity on the piston ring friction. The friction data showed good agreement with the Stribeck curve for the engine speed, in-cylinder pressure, and oil temperature changes.

KEY WORDS : Piston ring friction, Floating liner, Double pistons, Piston thrust force

1. INTRODUCTION

Now, global warming became a threat to the humanity. Unless the global greenhouse gas (GHG) emissions can be achieved a net-zero by 2050, additional warming will increase climate changes and may trigger tipping points. For decades, the main cause of GHG emissions has been the excessive use of fossil fuels. Internal combustion engines (ICEs), one of the most commonly used fuel-driven power systems, have faced the problem of maintenance or abolition. Many nations have attempted to convert ICEs into zero-emission vehicle systems. However, majority of the vehicles on actual roads still have ICEs. COP26 in Glasgow agreed on converting existing cars to zero-emission cars by 2035 (COP26 declaration on accelerating the transition to 100 % zero-emission cars and vans, 2021). Similar to the situation after the Paris Agreement in 2015, experts have determined that the total phase-out period of combustion cars is being prolonged by the capability gaps in the energy infrastructures between nations. Therefore, a contribution to the reduction in CO_2 emissions is still required for existing combustion cars.

Engine friction loss has constantly been an issue in improving fuel efficiency. Mechanical friction loss is inevitably linked to fuel consumption owing to the nature of engines with moving parts. Mechanical friction accounts for approximately 4 ~ 15 % of the total fuel energy for a typical estimate of friction for ICEs (Wong and Tung, 2016). The friction of the piston and piston ring system accounts for approximately 50 ~ 60 % of the total engine friction loss (Nakada, 1994). Majority of the piston assembly friction comes from either the (i) piston-skirt/ liner interaction, or (ii) ring-pack/liner interaction (Wong and Tung, 2016). Piston ring friction losses account for approximately 20 % of the total mechanical losses in modern ICEs (Smedley, 2004). Piston ring friction accounts for a significant amount of the total mechanical friction. Because piston rings are consumables, the piston friction loss can be improved by simply replacing the piston rings. Therefore, it is important to study piston ring friction.

Piston friction has been mainly studied because of its significant contribution to mechanical friction losses. It is complicated to analyze piston friction because it has a wide lubrication regime, from boundary friction to hydraulic friction. In addition, various factors affect this lubrication condition, including piston and ring designs, and environmental parameters such as engine oil temperature, engine speed, and in-cylinder pressure. To individually observe the effect of each factor on the piston friction, it is important to separate the piston friction from the other possible friction conditions for each component.

Several methodologies have been developed to capture only the piston friction. The most widely used method is engine strip-down. The strip-down method involves the literal removal of engine components one by one, and the comparison of the engine torque values before and after the disassembly of each part. Consequently, the friction torque of each engine component can be calculated. In addition,

**Corresponding author*. e-mail: kdmin@snu.ac.kr

indirect measurement methods can be used to observe piston lubricating conditions. The oil film thickness created between the ring surface and liner was measured as an indirect method to estimate the piston friction. Distance sensors and visualization methods using optical devices such as laser-induced fluorescence (LIF) can be adopted to measure oil film thickness. Furthermore, by measuring the axial force of the connecting rod, the piston friction force can be calculated using known values, comprising the gas force acting on the piston and inertia force. A strain gauge was attached to the connecting rod using wireless telemetry technology to measure the force of the connecting rod. By simply attaching the wireless strain gauge module to a conventional connecting rod, engine modifications can be greatly minimized (Fang *et al*., 2019). However, because of the device stability, these methods are challenging to utilize at engine firing conditions.

The floating liner method was introduced to conduct an in-depth study of the piston friction under both motoring and firing engine conditions. Dr. Shoichi Furuhama was the first to introduce this concept (Furuhama and Takiguchi, 1979). The principle of a floating-liner device is to suspend the liner in such a way that a number of piezoelectric load cells intervene at any point of contact between the liner and any rigidly mounted components (Gore *et al*., 2014). A conventional fixed liner is changed into a liner in a floating state, where the liner can be moved on a microscale. Therefore, the shear force created around the piston drags the liner up and down as the piston moves. Load cells capture the compression and extension force underneath the liner according to the linear movements. Stable piston friction data can be obtained using the floating-liner method under both motoring and firing engine conditions. However, because the floating liner engine from previous research uses a conventional piston-crank system, it captures not only the piston skirt and liner interaction, but also the piston ring-pack and liner interaction.

Separating the piston ring-pack friction from the piston friction has been attempted by several researchers. Furuhama and Takiguchi (1979) also introduced a different setup with a floating liner to measure only the piston ring friction. The cylinder head was then replaced with a guide. Another guide with a slightly smaller diameter was attached to the piston top. Relative to the guide mechanism, the guide was as long as possible to minimize the lateral motion of the piston. With this approach, only the piston ring friction can be measured. Other studies, including Cho *et al*. (2000), have also attempted a similar setup using this method. Söderfjäll *et al.* (2017) added another rod to one of the pistons of a six-cylinder engine. Therefore, the rod was connected to a piston ring holder. The rod is guided by a linear bearing to avoid contact between the test cylinder liner and ring holder. This means that piston ring friction can be isolated from other friction sources. The piston ring holder was inserted into a test cylinder, which was supported only via load cells, similar to the floating liner method. However, these methods were set up for a rig test of piston rings, and isolation of the piston ring friction under firing conditions has not been attempted.

To overcome this limitation in the previous studies, a new measurement system for piston ring friction was developed. By adding one more piston to the conventional piston-crank system, the new system can capture only the piston ring friction under both motoring and firing conditions. With the new measurement system, piston ring friction can be measured under various engine operating conditions. The experimental results show that the new system captures friction changes as the engine speed, oil temperature, and in-cylinder pressure change.

2. NEW MEASUREMENT SYSTEM FOR PISTON RING FRICTION

2.1. Double Pistons with Extended Connecting Rods

In contrast to the floating liner concept in previous studies, another piston was connected to the top of the conventional piston-crank system. To connect these two pistons, an extended connecting rod was assembled on top of a conventional piston. As shown in Figure 1, a liner for the lower piston was fixed as a conventional engine. A floating liner was placed on the upper piston and load cells were inserted underneath the floating liner. Therefore, the load cells measured the piston friction only at the upper piston.

By applying a new design concept, which is a double piston with an extended connecting rod, the piston thrust force can be significantly reduced compared to the conventional system. As shown in Figure 2, when the length of the connecting rod increased, the angle created by the connecting rod from the center of the crankshaft decreased. The upper piston has a much smaller angle (θ') than the lower piston (θ). Therefore, the thrust force acting on the upper piston can be reduced to approximately zero.

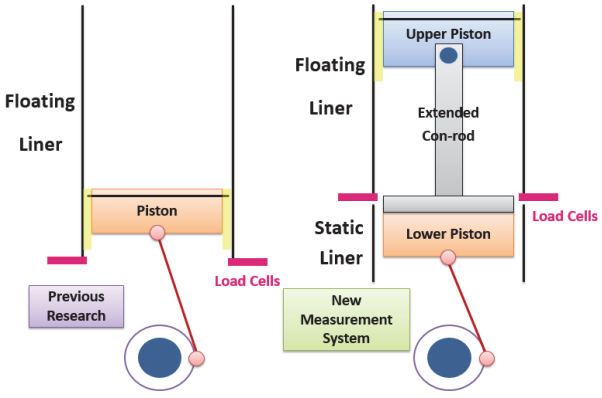

Figure 1. Schematic of a new measurement system and previous research.

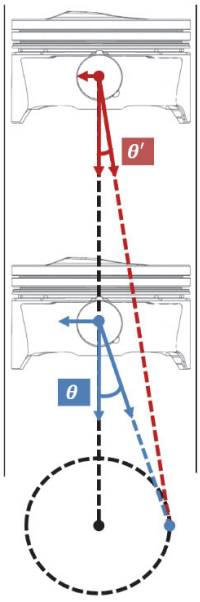

Figure 2. Piston force distribuation according to the distance between piston and crankshaft.

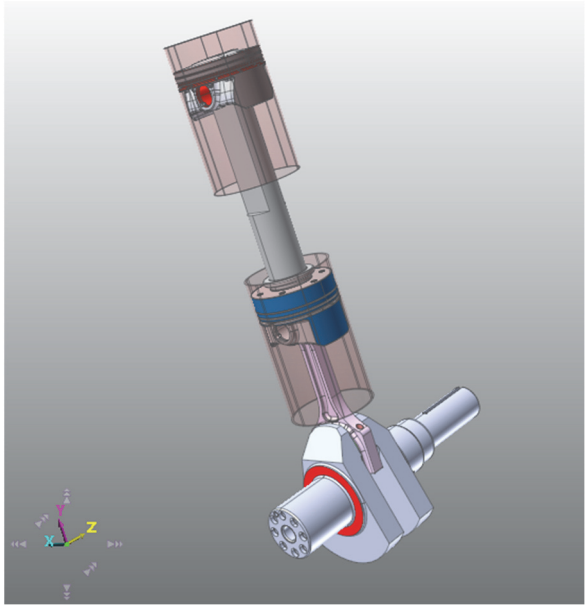

Figure 3. Dynamics simulation of the double piston engine using RecurDyn.

To verify the amount of thrust force in the 'double pistons' structure, a contact force between both pistons and liners have calculated using a simulation program. RecurDyn, a multi-body dynamics program, was used. The structural characteristics are shown in Figure 3 with the program. The measured in-cylinder gas pressure under the engine firing condition was used for the simulation. As plotted on Figure 4,

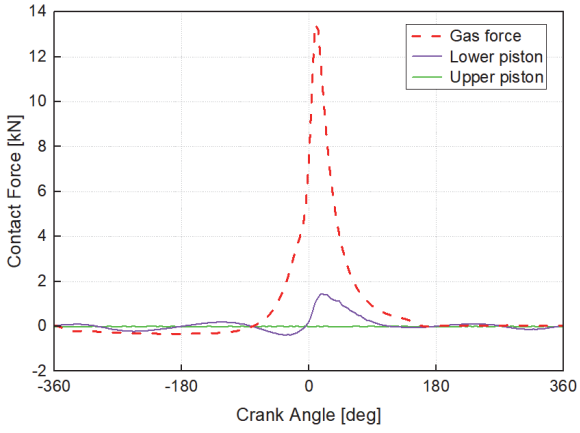

Figure 4. Dynamics simulation results – contact force between piston and liner at firing condition (700 rpm, IMEP 400 kPa).

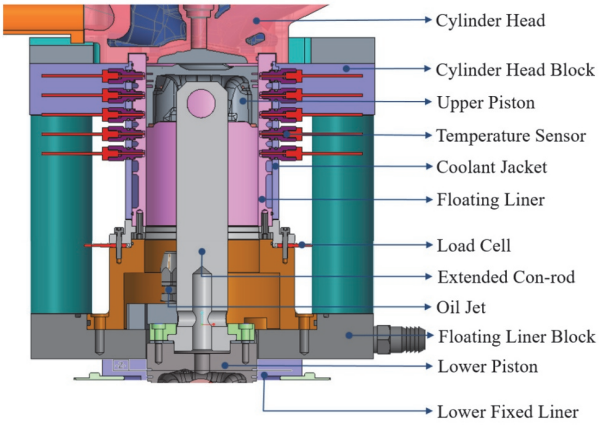

Figure 5. Piston ring friction measurement system – cross-sectional view.

the contact forces for the upper and lower pistons (X-axis indicated in Figure 3) can be calculated based on the gas force (Y-axis indicated in Figure 3) acting on the upper piston. The calculated contact force has positive and negative signs, which represent the force direction. A positive force indicates the force working towards the piston thrust side, similar to the engine exhaust, and a negative force indicates the opposite side of the engine intake. As shown in Figure 4, the thrust force on the upper piston was significantly smaller than the thrust force on the lower piston. The interactions between piston skirt and liner caused by piston thrust motion can be minimized with this 'double pistons' structure. Therefore, with the new system, it is possible to do more fundamental research on piston ring friction by excepting the friction from piston skirt (Oh, 2022).

Figure 5 shows the detailed view of the upper and lower pistons and extended con-rod. Each component of the cross-

sectional view is indicated in Figure 5. As shown on the figure, the extended con-rod is assembled on the top of the lower piston with blots. The center of the upper piston is synchronized with the lower piston. The upper piston cannot be lubricated properly as the scattered oil mist from crankshaft barely reaches through the end gaps of the lower piston. Therefore, the one another oil jet is added to lubricate the upper piston. The oil drain path is created through the extended con-rod and the lower piston for the oil residue.

2.2. In-cylinder Gas Sealing Method

To implement the experiment under the engine firing conditions, most importantly, the liner needs to be not only kept in a floating state but also thoroughly sealed for stable combustion. To compromise on these two opposite aspects, which maintain the liner floating state and simultaneously seal the in-cylinder gas, a new in-cylinder gas sealing method is applied.

Another gas seal was inserted between the cylinder head and the floating liner, as illustrated in Figure 6. When the gas chamber was pressurized, gas pressure was applied to the gas seal. The gas pressure makes the seal contact the inner surface of the floating liner, and the gas seal prevents the in-cylinder gas from leaking. During this process, the gas seal could generate extra friction on the floating liner, but a low-friction material was used. Furthermore, because of its dimensions, the effective contact area on the inner radial surface of the floating liner was negligibly small.

3. EXPERIMENTAL SETUP

3.1. Experimental Setup

A 523cc single cylinder engine was used as the base engine. The engine specifications are listed in Table 1. Because the engine has two pistons and liners, the engine specifications listed in Table 1 focus on the upper piston and liner. As seen on Figure 7, a double-piston-installed single-cylinder engine was set up on the test bed.

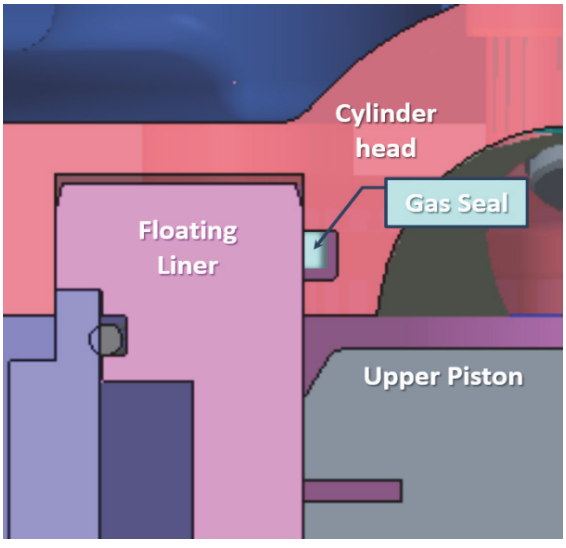

Figure 6. In-cylinder gas sealing method.

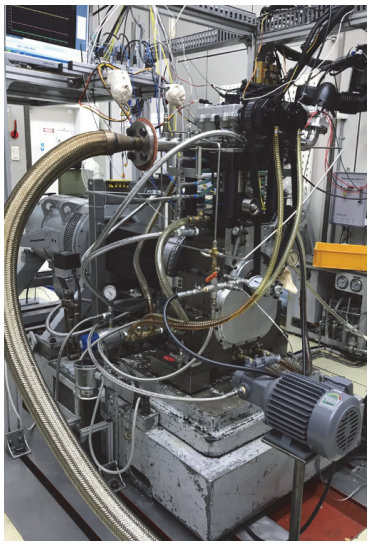

Figure 7. Measurement system set-up.

Table 1. Base engine specifications.

Engine type	Single cylinder SI engine
Displaced volume	523 cc
Bore × Stroke	88 mm × 86 mm
Compression ratio	10.5
Piston offset	0.8 mm
EVO EVC	bBDC 68° aTDC 1°
IVO IVC	aTDC 10° aBDC 67°
Max. valve lift	10 mm

The in-cylinder pressure was measured by a Kistler 6056A piezoelectric sensor, and the friction force was measured by four HBM CLP 7 kN washer-type piezoelectric load cells with HBM CMA amplifiers. A Kistler Kibox was used for high-frequency data acquisition. Load cells were placed at the engine front, rear, exhaust side, and inlet side. Thus, the position of each load cell was 90° when it was observed on top of the floating liner. By tightening the bolts for each washer-type load cell, nearly 2500 N is applied for each load cell as a pre-load. These signals are logged in Kistler Kibox To Go in every 0.1° crank angle.

Three piston rings were inserted in the piston for the experiment. The cross-sectional shape of the top compression ring (TCR) is rectangular and has a symmetric barrel face.

Table 2. Ring specifications.

	TCR	SCR	OCR
Tension [N]	8.9	8.0	27.9
Cross-sectional view			

Table 3. Experimental conditions.

Engine speed [rpm]	600 ~ 2000
Engine load [kPa]	IMEP 240 ~ 470
Oil temperature [°C] * SAE 5w-30 is used.	30, 60

The second compression ring (SCR) has a taper and balance under cutting. The oil control ring (OCR) consisted of three pieces: top and bottom plates, and a spacer. The tension values of all three rings are listed in Table 2.

3.2. Experimental Conditions

Three main parameters affecting piston ring friction were tested. The engine speed, load, and oil temperature were varied to observe the changes in the friction force using the newly invented measurement system. The experimental conditions are listed in Table 3. Coolant temperature is set the same with the oil temperature for each case.

4. RESULTS

The motoring and firing conditions were tested at various engine speeds, oil temperatures, and coolant temperatures. The engine speed and load were varied up to 2000 rpm and IMEP 470 kPa, respectively, excluding the natural frequency points of the engine. The motoring and firing conditions are plotted in Figure 8. Both experiments were performed at 700 rpm. As can be seen in the graph, the friction force has both positive and negative values. The value changes for every stroke and indicates the force direction. -360°, 0°, and 360°, were considered top dead centers (TDCs). 0° indicates the firing TDC for the firing cases. Similarly, -180° and 180° were considered bottom dead centers (BDCs). A compression stroke occurs from -180 to 0°; thus, the positive force value represents the compression force of the load cells.

As the in-cylinder pressure increased, the lubrication regime shifted according to the Stribeck curve. The boundary lubrication near the firing TDC, where the crank angle is 0°, shows the highest friction force compared to the other locations. The friction force at IMEP 400 kPa shows a higher value around firing TDC than that at motoring condition, for the in-cylinder pressure at IMEP 400 kPa condition is higher than that at the motoring condition. In addition, the friction force, especially at the compression and expansion strokes, shows that the force direction changes as the piston moving direction. The experimental result for the firing case implies that the piston thrust force was minimized. Thus, piston lateral motion did not affect the friction measurement. As a result, changes in piston ring friction were specifically observed in this research.

Similarly, various engine load conditions were tested at 700 rpm, and the results are shown in Figure 9. Figure 9 also shows the effect of the in-cylinder gas pressure on the piston ring friction force. As the gas pressure increased, the lubrication condition shifted towards the boundary lubrication regime. Thus, the friction force near the firing TDC increases as cylinder pressure peak increases considerably from IMEP 240 kPa case to IMEP 470 kPa case.

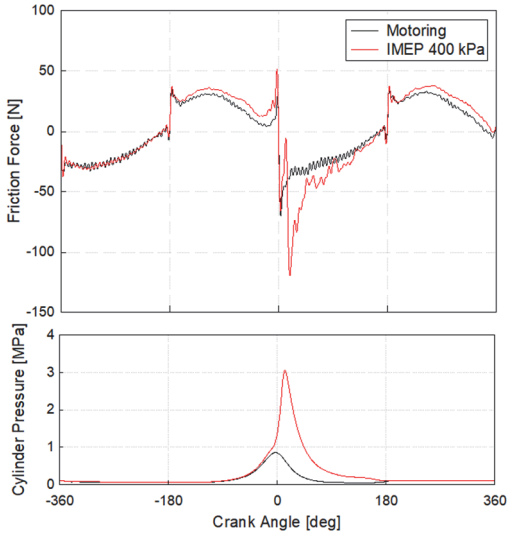

Figure 8. Friction force at motoring/firing conditions.

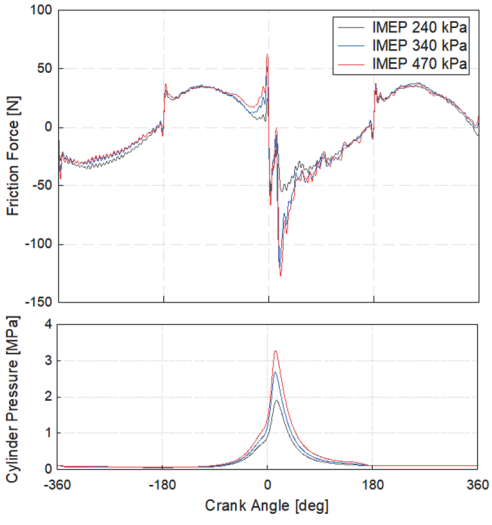

Figure 9. Friction force at various firing conditions.

Moreover, the friction force exhibited different characteristics at various engine speeds under motoring conditions. The change in engine speed is directly related to that in piston speed. When the piston speed increased, the piston ring friction lubrication regime tended to move towards the hydrodynamic lubrication regime. As seen in Figure 10, the friction force at the boundary lubrication decreases with an increase in the engine speed near the dead centers, where the piston speed becomes zero. For the hydrodynamic lubrication zone, the 2000 rpm case shows a higher friction force than the 700 rpm case.

With the new measurement system, the gas pressure effect at the top of the piston could be eliminated and tested. Under engine motoring conditions, but without pressure, the oil temperature effect can be observed.

Two different oil temperatures were tested to determine the effect of the oil viscosity on the piston friction, and coolant temperature is set the same as the oil temperature. Oil temperatures of 30 °C and 60 °C were recorded at 700 rpm. As the oil temperature increased, the oil viscosity exponentially decreased. In addition, the lubrication regime changed. As plotted in Figure 11, the boundary friction force near the TDCs and BDCs increased as the oil viscosity decreased. On the other hand, the hydraulic friction force between the TDC and BDC decreased as the oil viscosity decreased. When the oil temperature increases, the oil tends to flow rather than attach to the liner wall because of its low viscosity. Therefore, the oil pressure is not sufficiently high to prevent metal-to-metal contact when the piston speed is low, such as at TDCs and BDCs. Because the oil film is thinner, the hydraulic shear stress is lower at the position between the TDC and the BDC.

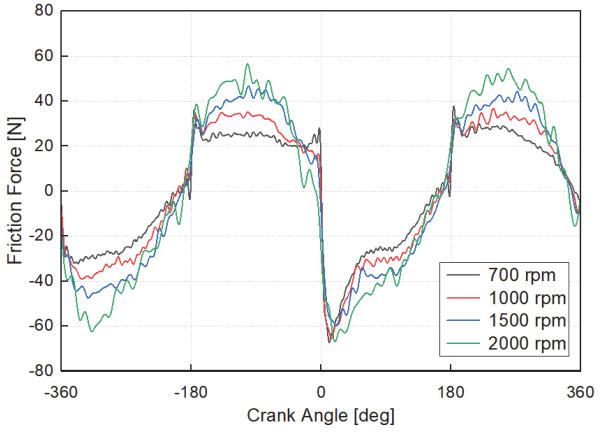

Figure 10. Friction force at various engine speeds.

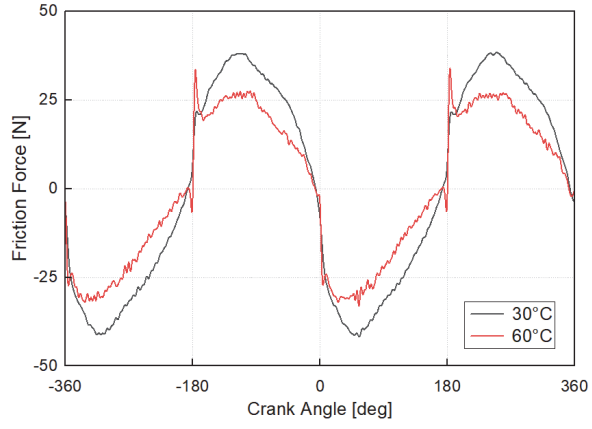

Figure 11. Friction force at various oil temperatures.

5. CONCLUSION

The floating liner method is useful for investigating piston friction in various engine operating conditions including engine motoring and firing conditions without any modification of engine geometry. However, it remains challenging to exclude the lateral piston force effects from the measured data. In this study, the piston secondary motion from the angle created between the connecting rod and piston center is highly reduced to measure the friction force from only the piston rings. Therefore, a double-piston structure was adopted, which is different from the conventional engine structure for the floating liner method. The experimental results show the piston ring friction data, and they are in good agreement with the base theory at various cylinder pressures and oil temperatures.

(1) With the measurement data at the various in-cylinder pressure, the engine load effect on piston ring friction can be observed. As the in-cylinder pressure increases for higher engine load, the lubrication regime especially near the firing TDC tends to shift towards the boundary lubrication. The friction force increases as the in-cylinder pressure increases. The maximum friction force occurs when the pressure reaches peak.

(2) To confirm the piston speed effect on piston ring friction, the engine speed was varied from 700 rpm to 2000 rpm in the experiment. As the piston speed varied within each stroke, the hydrodynamic lubrication regime shows the visible friction changes with different engine speeds. When the piston speed reaches the highest near the middle of the stroke, the lubrication regime shifts to hydrodynamic lubrication condition. Therefore, when the piston speed increases with the engine speed, the piston ring friction increases in the middle of each stroke.

(3) Two different oil viscosities were tested by varying oil temperature. Oil viscosity contributes to the remaining oil amount on the liner. When the oil temperature increases from 30 °C to 60 °C, the oil film created on the liner becomes thinner with increased fluidity. The thin oil film creates the higher friction at the boundary lubrication condition and the lower friction at the hydrodynamic lubrication condition.

Although the newly developed measurement system for piston ring friction has proven its ability to track frictional changes, there is still a room for further improvement to obtain more reliable data. Two main improvements will be discussed in future work. First, a system that can change only the piston and piston ring from the engine is considered to achieve improved repeatability of each experiment. Second, the extra force factors that affect the measurement of only the piston ring friction will be checked and removed further.

ACKNOWLEDGEMENT–This research was supported by the Hyundai Motor Group, Korea Piston Ring Inc. (KPR), and Seoul National University, Institute of Advanced Machinery and Design (SNU-IAMD).

REFERENCES

Cho, S. W., Choi, S. M. and Bae, C. S. (2000). Frictional modes of barrel shaped piston rings under flooded lubrication. *Tribology International* **33**, **8**, 545–551.

COP26 declaration on accelerating the transition to 100 % zero emission cars and vans (2021). https://www.gov.uk/government/publications/cop26-declaration-zero-emission-cars-and-vans/cop26-declaration-on-accelerating-the-transition-to-100-zero-emission-cars-and-vans

Fang, C., Meng, X., Xie, Y., Wen, C. and Liu, R. (2019). An improved technique for measuring piston-assembly friction and comparative analysis with numerical simulations: Under motored condition. *Mechanical Systems and Signal Processing*, **115**, 657–676.

Furuhama, S. and Takiguchi, M. (1979). Measurement of piston frictional force in actual operating diesel engine. *SAE Transactions*, 2896–2914.

Gore, M., Theaker, M., Howell-Smith, S., Rahnejat, H. and King, P. D. (2014). Direct measurement of piston friction of internal-combustion engines using the floating-liner principle. *Proc. Institution of Mechanical Engineers, Part D: J. Automobile Engineering* **228**, **3**, 344–354.

Nakada, M. (1994). Trends in engine technology and tribology. *Tribology Int.* **27**, **1**, 3–8.

Oh, H. (2022). *Development of a New Measurement System for Piston Ring Friction*. Seoul National University.

Smedley, G. (2004). *Piston Ring Design for Reduced Friction in Modern Internal Combustion Engines.* Doctoral Dissertation. Massachusetts Institute of Technology.

Söderfjäll, M., Herbst, H. M., Larsson, R. and Almqvist, A. (2017). Influence on friction from piston ring design, cylinder liner roughness and lubricant properties. *Tribology Int.*, **116**, 272–284.

Wong, V. W. and Tung, S. C. (2016). Overview of automotive engine friction and reduction trends–Effects of surface, material, and lubricant-additive technologies. *Friction*, **4**, 1–28.